

# Optimized Parallel Coding of Second-Order Stimulus Features by Heterogeneous Neural Populations

Chengjie G. Huang and Maurice J. Chacron

Department of Physiology, McGill University, Montreal, Quebec H3G 1Y6, Canada

Efficient processing of sensory input is essential to ensure an organism's survival in its natural environment. Growing evidence suggests that sensory neurons can optimally encode natural stimuli by ensuring that their tuning opposes stimulus statistics, such that the resulting neuronal response contains equal power at all frequencies (i.e., is “white”). Such temporal decorrelation or whitening has been observed across modalities, but the effects of neural heterogeneities on determining tuning and thus responses to natural stimuli have not been investigated. Here, we investigate how heterogeneities in sensory pyramidal neurons organized in three parallel maps representing the body surface determine responses to second-order electrosensory stimulus features in the weakly electric fish *Apteronotus leptorhynchus*. While some sources of heterogeneities such as ON- and OFF-type responses to first-order did not affect responses to second-order electrosensory stimulus features, other sources of heterogeneity within and across the maps strongly determined responses. We found that these cells effectively performed a fractional differentiation operation on their input with exponents ranging from zero (no differentiation) to 0.4 (strong differentiation). Varying adaptation in a simple model explained these heterogeneities and predicted a strong correlation between fractional differentiation and adaptation. Using natural stimuli, we found that only a small fraction of neurons implemented temporal whitening. Rather, a large fraction of neurons did not perform any significant whitening and thus preserved natural input statistics in their responses. We propose that this information is needed to properly decode optimized information sent in parallel through temporally whitened responses based on context.

**Key words:** adaptation; electrosensory; envelope; neural coding; SK channels; weakly electric fish

## Significance Statement

We demonstrate that heterogeneities in the same sensory neuron type can either have no or significant influence on their responses to second-order stimulus features. While an ON- or OFF-type response to first-order stimulus attributes has no significant influence on responses to second-order stimulus features, we found that only a small fraction of sensory neurons optimally encoded natural stimuli through high-pass filtering, thereby implementing temporal whitening. Surprisingly, a large fraction of sensory neurons performed little if no filtering of stimuli, thereby preserving natural stimulus statistics. We hypothesize that this pathway is necessary to properly decode optimized information contained in temporally whitened responses based on context.

## Introduction

Understanding how the brain processes sensory input, thereby leading to behavior (i.e., the neural code), remains a central problem in neuroscience. Growing evidence suggests that the brain's

coding strategies are adapted to the statistics of stimuli found in the natural environment, thereby making the use of natural stimuli paramount toward understanding the neural code (Attneave, 1954; Barlow, 1961; Laughlin, 1981; Simoncelli and Olshausen, 2001). In particular, it has been proposed that sensory neurons can efficiently encode time-varying natural stimuli by removing redundant information and therefore maximizing information transmission (Rieke et al., 1996), leading to a neural response with equal power at all frequencies (i.e., “white”). Experiments have provided evidence that sensory neurons achieve such temporal decorrelation or whitening of natural stimuli by matching their tuning properties to natural stimulus statistics across modalities [visual (Dan et al., 1996; Wang et al., 2003), auditory (Rodríguez et al., 2010), somatosensory (Pozzorini et al., 2013),

Received April 28, 2016; revised July 14, 2016; accepted Aug. 9, 2016.

Author contributions: M.J.C. designed research; C.G.H. performed research; C.G.H. analyzed data; C.G.H. and M.J.C. wrote the paper.

This work was supported by the Fonds de recherche du Québec–Nature et Technologies and the Canada Research Chairs (M.J.C.).

The authors declare no competing financial interests.

Correspondence should be addressed to Dr. Maurice J. Chacron, McIntyre Medical Research Building, Room 1137, 3655 Promenade Sir William Osler, Montreal, QC H3G 1Y6, Canada. E-mail: maurice.chacron@mcgill.ca.

DOI:10.1523/JNEUROSCI.1433-16.2016

Copyright © 2016 the authors 0270-6474/16/369859-14\$15.00/0

electrosensory (Huang et al., 2016)]. However, strong heterogeneities have been observed in neural populations (Bannister and Larkman, 1995a,b; Goldberg, 2000), even for a given cell type (Marder and Goaillard, 2006; Schulz et al., 2006). While heterogeneities can benefit coding (Padmanabhan and Urban, 2010; Mejias and Longtin, 2012; Tripathy et al., 2013), how these influence optimized coding of natural stimuli through temporal whitening has not been investigated to date.

Gymnotiform wave-type weakly electric fish offer an attractive model system for studying the coding of natural stimuli because of their well-characterized neural circuits and natural stimulus statistics. These fish sense amplitude modulations (AMs) of their self-generated quasi-sinusoidal electric organ discharge (EOD) through peripheral electroreceptors found on their skin. Electroreceptors send afferents that trifurcate to contact sensory pyramidal neurons within three parallel maps of the body surface [the lateral segment (LS), centrolateral segment (CLS), and centromedial segment (CMS)] within the electrosensory lateral line lobe (ELL) that subsequently project to higher brain areas, thereby mediating perception and behavioral responses (for review, see Chacron et al., 2011; Marsat et al., 2012; Krahe and Maler, 2014). ELL pyramidal cells display large and well-known heterogeneities. First, there are two pyramidal cell types: ON cells that respond to increases in EOD amplitude and OFF cells that instead respond to decreases in EOD amplitude (Saunders and Bastian, 1984). Second, pyramidal cells within a given map display large heterogeneities in both morphology and physiology (Bastian and Nguyenkim, 2001; Bastian et al., 2002, 2004; Chacron et al., 2005a,b; Chacron, 2006; Avila-Akerberg et al., 2010). Third, pyramidal cells across the three ELL maps display strong response heterogeneities (Shumway, 1989; Krahe et al., 2008).

As in other sensory modalities, natural electrosensory stimuli consist of a fast time-varying waveform (i.e., the EOD AM which is a first-order attribute) whose amplitude (i.e., the envelope which is a second-order attribute) varies more slowly (Stamper et al., 2013). It is important to note that the animal's EOD is a carrier and that the time-varying EOD AM is the meaningful stimulus here. Thus, the first- and second-order features of the stimulus correspond to the second- and third-order features of the full signal received by the animal, respectively. Envelopes carry behaviorally relevant information and are processed within the brain as they give rise to behavioral responses (Stamper et al., 2012; Metzen and Chacron, 2014). While much is known about how heterogeneities in ELL pyramidal cells influence responses to AMs (for review, see Maler, 2009; Krahe and Maler, 2014), almost nothing is known about their influence on responses to envelopes. ELL pyramidal cells can respond to envelopes (Middleton et al., 2006; McGillivray et al., 2012), and a previous study showed that LS pyramidal cells efficiently process envelopes through temporal whitening by matching their tuning properties to natural statistics (Huang et al., 2016). However, the effects of pyramidal cell heterogeneities within as well as across the ELL maps on their responses to envelopes have not been investigated to date.

## Materials and Methods

**Animals.** The weakly electric fish *Apteronotus leptorhynchus* was used exclusively in this study. Animals of either sex were purchased from tropical fish suppliers and were acclimated to laboratory conditions according to published guidelines (Hitschfeld et al., 2009). All procedures were approved by McGill University's animal care committee and were

performed in accordance with the guidelines of the Canadian Council on Animal Care.

**Surgery.** Surgical procedures have been described in detail previously (Chacron et al., 2003; Toporikova and Chacron, 2009; Metzen et al., 2015). Briefly, 0.1–0.5 mg of tubocurarine (Sigma) was injected intramuscularly to immobilize the fish for electrophysiology experiments. The fish was respired through a mouth tube at a flow rate of ~10 ml/min when placed in the recording tank. To stabilize the head during electrophysiology recordings, a metal post was glued to the exposed area of the skull. A small hole of ~2 mm<sup>2</sup> was drilled over the caudal lobe of the cerebellum above the ELL to gain access to the pyramidal neurons.

**Electrophysiology.** We used well-established techniques to perform extracellular recordings with Woods metal electrodes from pyramidal cells (Frank and Becker, 1964). Cells were assigned to each segment based on recording depth and mediolateral placement of the electrode on the brain surface as done previously (Krahe et al., 2008; Khosravi-Hashemi and Chacron, 2014). Extracellular recordings were digitized using CED 1401-plus hardware and Spike II software at 10 kHz sampling rate.

**Stimulation.** The electric organ discharge of *A. leptorhynchus* is neurogenic, and therefore is not affected by injection of curare. All stimuli consisted of AMs of the animal's own EOD and were produced by triggering a function generator to emit one cycle of a sine wave for at each zero crossing of the EOD as done previously (Bastian et al., 2002). The frequency of the emitted sine wave was set slightly higher (~30 Hz) than that of the EOD, which allowed the output of the function generator to be synchronized to the animal's discharge. The emitted sine wave was subsequently multiplied with the desired AM waveform (MT3 multiplier; Tucker Davis Technologies), and the resulting signal was isolated from the ground (A395 linear stimulus isolator; World Precision Instruments). The isolated signal was then delivered through a pair of chloridized silver wire electrodes placed ~15 cm away from the animal on either side of the recording tank perpendicular to the fish's rostral-caudal axis. Depending on polarity, the isolated signal either added or subtracted from the animal's own discharge. The stimulus intensity was adjusted to give rise to changes in EOD amplitude that were ~20% of the baseline level as in previous studies (Deemyad et al., 2013; Aumentado-Armstrong et al., 2015; Simmonds and Chacron, 2015; Metzen et al., 2016), as measured using a small dipole placed close to the animal's skin. The typical stimulus intensity used was ~0.2 mV/cm. The stimuli consisted of a 4 Hz sine wave AM with a constant envelope to test pyramidal cell responses to first-order stimuli. Moreover, we used stimuli consisting of two noisy AM waveforms with frequency contents of 5–15 and 60–80 Hz whose envelopes were modulated sinusoidally with frequencies ranging from 0.05 to 1 Hz, mimicking those frequencies found in movement envelopes (Metzen and Chacron, 2014, 2015; Huang et al., 2016). We also used noisy envelopes whose spectrum decayed as a power law with exponent -0.8 mimicking signals seen under natural conditions (Metzen and Chacron, 2014).

**Fractional differentiation model.** Fractional differentiation is a linear operation that can be described simply as  $d^\alpha/dt^\alpha$ , in which the order of differentiation  $\alpha$  is a noninteger number. In the frequency domain, fractional differentiation of order  $\alpha$  corresponds to filtering by a transfer function  $H(f)$  given by the following:

$$H(f) = (2\pi f)^\alpha \exp\left(i \frac{\alpha\pi}{2}\right).$$

The gain  $G(f)$  and phase  $\phi(f)$  of the model can then be written as follows:

$$G(f) = |H(f)| = (2\pi f)^\alpha,$$

$$\phi(f) = \arctan\left(\frac{\text{Im}[H(f)]}{\text{Re}[H(f)]}\right) = \frac{\alpha\pi}{2},$$

where  $\text{Im}[H(f)]$  and  $\text{Re}[H(f)]$  are the imaginary and real parts, respectively. We fitted a fractional differentiation model to our data using the

Grunwald–Letnikov definition, which was adapted to use a vectorization method to pass signals through a spectrum of fractional derivative values between 0 and 1 from which we obtained the fractional differential exponent  $\alpha_{\text{neuron}}$ .

**Neuron model.** To model the pyramidal neural responses to the stimuli used in this study, we implemented a leaky integrate-and-fire (LIF) model (Lapicque, 1907) with a power-law adaptation:  $C(dV/dt) = -g_{\text{leak}}(V - E_{\text{leak}}) - z_1(t) + I + \sigma_{\text{noise}}\xi(t) + \sigma_{\text{stim}}s(t)$ , where  $C$  is the membrane capacitance,  $g_{\text{leak}}$  is the leak conductance,  $E_{\text{leak}}$  is the leak reversal potential,  $I$  is a constant bias current,  $\xi(t)$  is Gaussian white noise with zero mean and standard deviation unity,  $\sigma_{\text{noise}}$  is the noise intensity,  $s(t)$  is the stimulus which was taken to have the same statistics as for the data,  $\sigma_{\text{stim}}$  is the stimulus intensity,  $V$  is the membrane potential, and  $z_1(t)$  is the adaptation current. Each time the membrane potential reaches the threshold  $\theta$ , it is reset to  $V_{\text{reset}}$  and an action potential is said to have occurred at that time. We approximated the power-law adaptation using  $M$  variables  $z_1 \dots z_M$  that obeyed the following system of differential equations (Drew and Abbott, 2006):

$$\frac{dz_i}{dt} = \frac{-z_i(t) + z_{i+1}(t)}{\tau_i} + b\gamma^{i-1} \sum_j \delta(t - t_j) \quad \text{for } i = 1 \text{ to } M - 1,$$

$$\frac{dz_M}{dt} = \frac{-z_M(t)}{\tau_M} + b\gamma^{M-1} \sum_j \delta(t - t_j),$$

$$\tau_i = \tau_{\text{min}} \gamma^{i-1},$$

where  $t_j$  are the spikes times,  $\delta(t)$  is the delta function, and  $b$  and  $\gamma$  are constants that determine the strength and power-law exponent  $\alpha_{\text{neuron}}$  of the neural sensitivity, respectively. The model was simulated using an Euler–Maruyama integration with time step  $dt = 0.025$  ms. Unless stated otherwise, we used parameter values  $C = 1 \mu\text{F}/\text{cm}^2$ ,  $g_{\text{leak}} = 0.36 \mu\text{S}/\text{cm}^2$ ,  $E_{\text{leak}} = -70$  mV,  $I = 7 \mu\text{A}/\text{cm}^2$ ,  $\sigma_{\text{noise}} = 5 \mu\text{A}/\text{cm}^2$ ,  $M = 40$ ,  $b = 0.2$ ,  $\gamma = 1.1253$ ,  $\tau_{\text{min}} = 100$  ms,  $\theta = -50$  mV,  $V_{\text{reset}} = -70$  mV, and  $C = 1 \mu\text{F}/\text{cm}^2$ . We note that we varied parameters  $b$  (the adaptation strength) as well as  $I$  (the bias current) to reproduce the heterogeneities seen across segments as well as within each segment when considering the different cell classes (i.e., superficial, intermediate, and deep).

**Data analysis.** Superficial, intermediate, and deep pyramidal cells were segregated based on the baseline (i.e., in the absence of stimulation but in the presence of the animal's unmodulated EOD) firing rate, as done previously (Chacron et al., 2005b; Chacron, 2006; Avila-Akerberg et al., 2010). Cells whose baseline firing rate was less or equal to 15 Hz were classified as superficial, cells whose baseline firing rate was greater or equal to 35 Hz were classified as deep, cells whose baseline firing rate was between 15 and 35 Hz were classified as intermediate.

To quantify the neural responses and relate them to the stimulus envelope, we used linear systems identifications techniques to compute the gain and phase relationships. The recorded membrane potential was first high-pass filtered (100 Hz; eighth-order Butterworth). Spike times were defined as the times at which this signal crossed a given threshold value from below. A binary sequence  $R(t)$  was constructed from the spike times by discretizing time into bins of 0.1 ms width and setting the content of a given bin to 10,000 if a spike occurred within it or 0 otherwise. The time-varying firing rate was obtained by low-pass filtering  $R(t)$  using a second-order Butterworth filter with cutoff frequencies 0.2, 0.35, 0.75, 1.5, 2.5, and 3.5 Hz for envelope frequencies 0.05, 0.1, 0.2, 0.5, 0.75, and 1 Hz, respectively. Using linear systems identification techniques, the response gain was calculated as the ratio of the amplitude of the filtered firing rate response and the amplitude of the stimulus obtained from the dipole during the recording. The response phase was calculated as the average phase at which the filtered firing rate waveform reached its maximum value relative to the peak values of the stimulus waveform over each cycle/period of  $2\pi$ . We note that computing response gain from the phase histogram gave values that were not significantly different than those obtained using the filtered firing rate (data not shown).

The whitening index was calculated by taking the area under the power spectrum curve of the spiking response using a trapezoidal method and dividing by that obtained by replacing all values by the maximum value in

the power spectrum. The whitening index ranges between 0 and 1, where 1 indicates complete whitening (i.e., a power spectrum that is independent of temporal frequency), as done previously (Huang et al., 2016).

## Results

We recorded from ELL pyramidal cells within the CMS, CLS, and LS maps. Our stimuli consisted of sinusoidal AMs with constant amplitude as well as noisy EOD AMs whose envelope (1) varied sinusoidally at different frequencies spanning the behaviorally relevant range or (2) mimicked the frequency spectrum of natural envelopes. Figure 1A shows example traces of the AM (magenta), envelope (blue), and the full signal received by the animal (green) with their respective temporal frequency contents. Previous results have shown that cells whose somata are found most superficially within the pyramidal cell layer (i.e., superficial pyramidal cells) tend to have the largest dendritic trees. In contrast, cells whose somata are found most deeply within the pyramidal cell layer (i.e., deep pyramidal cells) tend to have the smallest dendritic trees. Finally, cells whose somata are located at intermediate levels within the pyramidal cell layer (i.e., intermediate pyramidal cells) have properties in between those of their superficial and deep counterparts. Importantly, previous anatomical work has shown that ELL pyramidal cells are organized in columns within each map (Maler, 2009). Each column consists of six cells (ON- and OFF-type deep, intermediate, and superficial) receiving almost identical input from peripheral receptors (Fig. 1B). Previous studies have shown a strong correlation between the baseline (i.e., in the absence of stimulation) firing rate and the location of the soma within the pyramidal cell layer (Bastian and Nguyenkim, 2001; Bastian et al., 2004). We thus used the baseline firing rate to distinguish between these cell classes, as done previously (Chacron et al., 2005b; Chacron, 2006; Avila-Akerberg et al., 2010).

### ON- and OFF-type pyramidal neurons display similar responses to envelopes

We first investigated how ON- and OFF-type ELL pyramidal cells responded to EOD AMs. ON- and OFF-type pyramidal cells have different morphologies and can easily be distinguished based on their responses to AM stimuli (Maler, 1979; Maler et al., 1981; Saunders and Bastian, 1984; Bastian et al., 2002). Indeed, in the case of a 4 Hz sinusoidal AM, ON-type cells tend to respond during the stimulus upstroke and near the peak (Fig. 2A). In contrast, OFF-type cells tend to respond during the stimulus downstroke and near the trough (Fig. 2B). As such, ON-type ( $n = 46$ ) and OFF-type ( $n = 45$ ) cells in our data set responded to opposite phases (Fig. 2C,D) of the AM. The distribution of preferred phases of all recorded neurons was clearly bimodal (Hartigan's dip test,  $p = 0.01$ ; Fig. 2E), consistent with previous results (Saunders and Bastian, 1984; Bastian et al., 2002).

We next investigated how ON- and OFF-type ELL pyramidal cells responded to envelopes. Surprisingly, we found that both ON- and OFF-type ELL pyramidal cells displayed similar responses (Fig. 3A,B) to these by firing preferentially during the envelope upstroke (Fig. 3C,D). Similar results were seen across our data set as the distributions of preferred phases largely overlapped between ON and OFF cells (Fig. 3E). Similar sensitivity and phases for envelope responses were observed when using either low-frequency (5–15 Hz) or high-frequency (60–80 Hz) AMs (Kruskal–Wallis test,  $p = 0.85$ ). Responses obtained for either low- or high-frequency AMs were thus pooled in all subsequent analyses. We conclude that ON- and OFF-type



pyramidal cells, despite responding in opposite fashion to AMs, actually respond similarly to envelopes.

**Pyramidal cell populations of different ELL segments display differential tuning to envelopes**

Previous studies have shown important differences between the responses of ELL pyramidal cells across the three maps to AM stimuli (Shumway, 1989; Krahe et al., 2008; Mehaffey et al., 2008) and have suggested different functional roles for each map (Metzner and Juranek, 1997). Thus, one possibility is that one ELL map is specialized to process envelope stimuli. If that were the case, then we would expect that only pyramidal neurons within that map would respond to envelopes. Another possibility is that ELL pyramidal neurons across the three maps are tuned differentially to envelopes, as is observed for AMs (Shumway, 1989; Krahe et al., 2008).

We thus investigated how ELL pyramidal cells within the LS (ON,  $n = 21$ ; OFF,  $n = 14$ ), CLS (ON,  $n = 15$ ; OFF,  $n = 14$ ), and CMS (ON,  $n = 12$ ; OFF,  $n = 15$ ) maps respond to envelopes. Since sinusoidal envelope stimulation elicited sinusoidal modulations in firing rate at the same frequency, we used linear systems identification techniques (see Materials and Methods) to quantify the gain and phase relationship between the envelope and neural response. We found that for both ON- and OFF-type LS pyramidal cells, gain increased as a power law as a function of increasing envelope frequency (Fig. 4A, green and red filled circles), while phase was largely independent of envelope frequency (Fig. 4A, green and red open circles), which is characteristic of fractional differentiation (Lundstrom et al., 2008; Pozzorini et al., 2013). We thus fitted a fractional differentiation model to our data (see Materials and Methods) and found excellent agreement (Fig. 4A, compare circles, dashed lines). We obtained similar fractional differentiation exponents (which is equal to the power-law exponent describing the increase in gain) for ON- and OFF-type LS pyramidal cells (ON,  $\alpha = 0.31 \pm 0.04$ ; OFF,  $\alpha = 0.27 \pm 0.04$ ; one-way ANOVA,  $p = 0.52$ ).

We found qualitatively similar results for CLS pyramidal cells in that the gain also increased as a power law as a function of increasing envelope frequency and that the phase lead was also independent of envelope frequency for both ON- and OFF-type CLS neurons (Fig. 4B, compare filled, open red and green circles). Our data for the CLS pyramidal cells were also well fit by a fractional differentiation model (Fig. 4B, compare circles, dashed lines). However, we

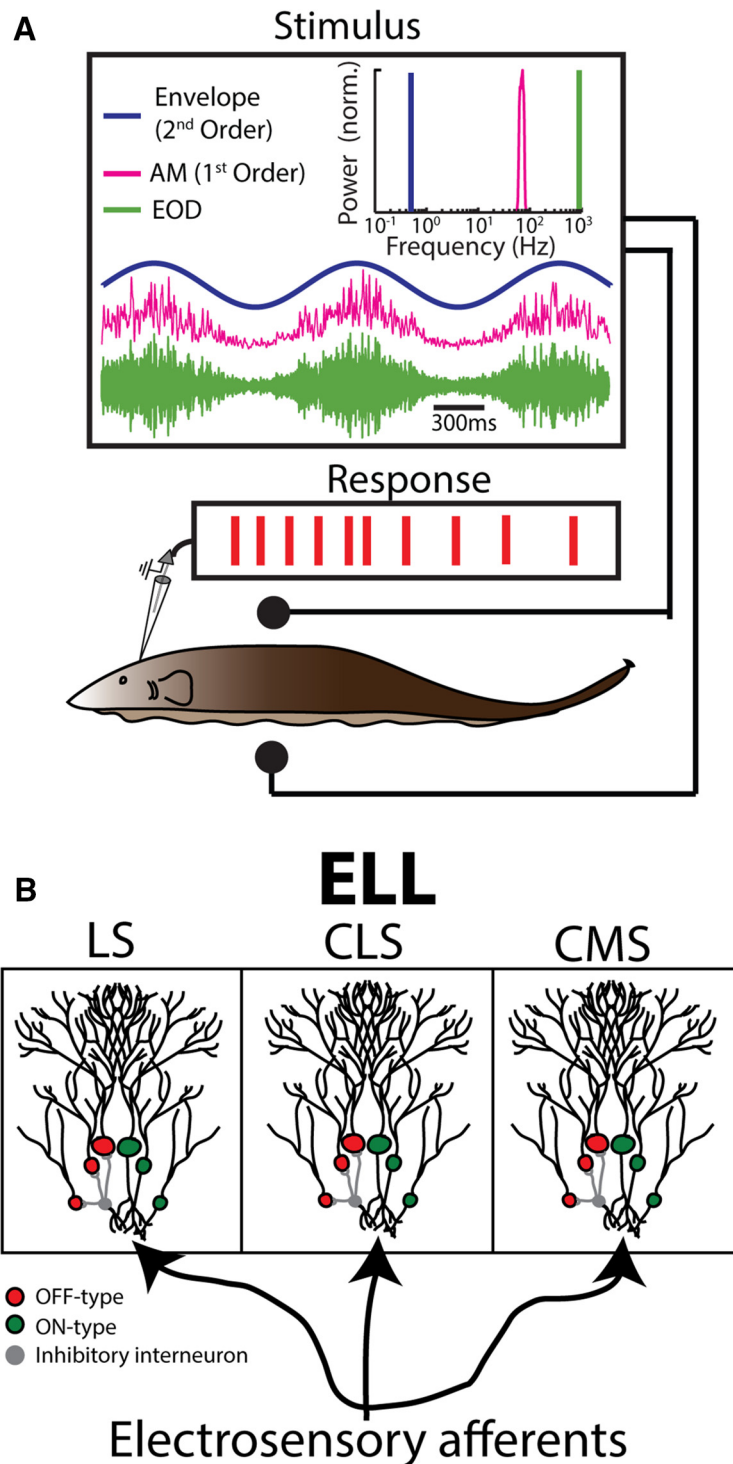


**Figure 1.** Experimental setup and relevant anatomy. *A*, Schematic representation showing the awake-behaving preparation where a stimulus is presented to the animal while neural activity is being recorded via extracellular Woods metal electrodes. Shown on the right are an example AM waveform (magenta), its envelope (blue), and the full signal received by the animal (green) with their respective frequency contents. *B*, Schematic showing anatomy where peripheral electrosensory afferents trifurcate to make synaptic contact with pyramidal cells with three parallel maps of the body surface: the lateral segment, the centrolateral segment, and the centromedial segment. Within each segment, pyramidal cells are organized into columns each consisting of six cells: three ON-type cells (deep, intermediate, superficial) and three OFF-type cells (deep, intermediate, superficial).

found that the rate of increase of the gain as well as the phase lead were smaller in magnitude than those observed for LS pyramidal cells, as confirmed by smaller fractional differentiation exponents that were similar for ON- and OFF-type cells but lower than those

# AMs

## A ON-type Pyramidal Cell    B OFF-type Pyramidal Cell

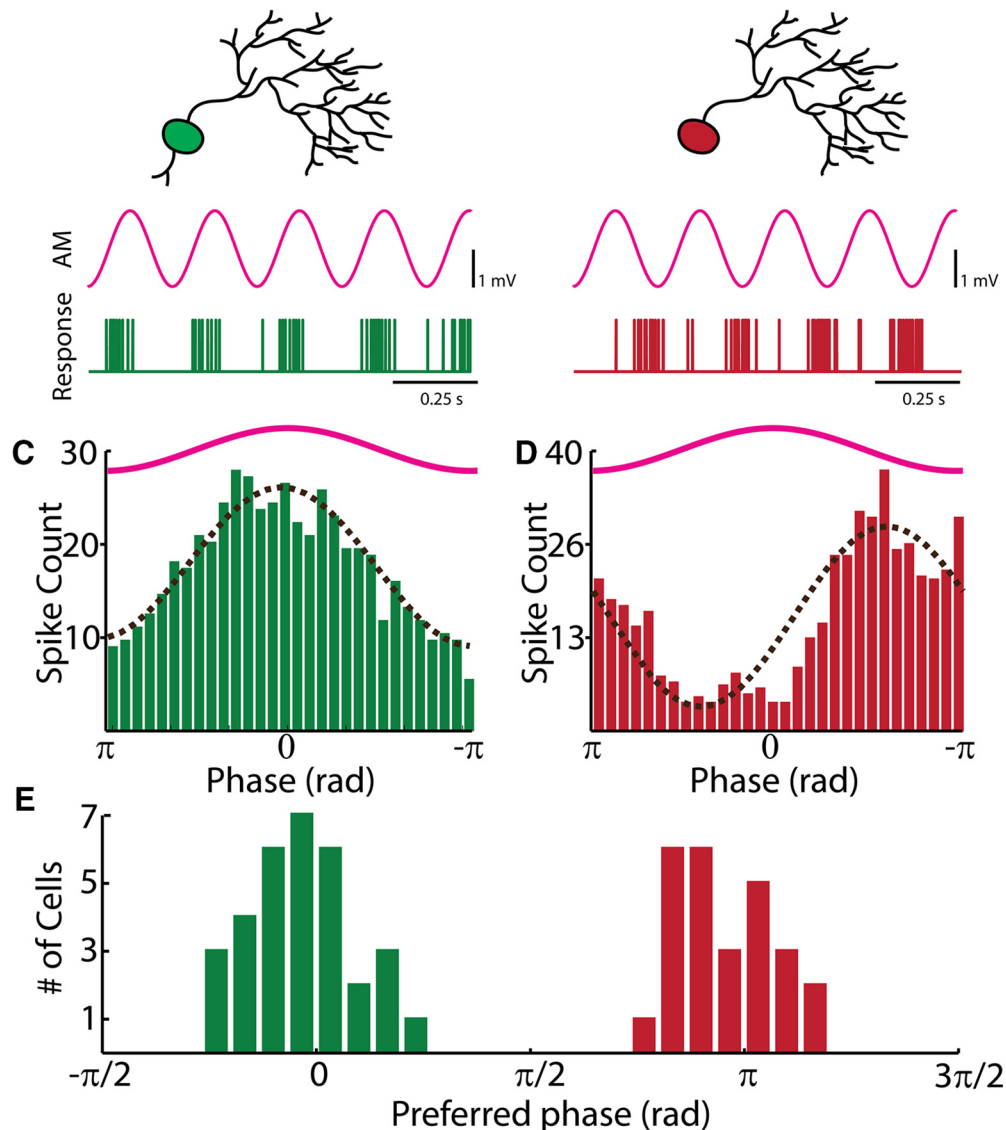


**Figure 2.** ON- and OFF-type pyramidal neurons respond in opposite fashions to EOD AMs (i.e., first order). **A**, Top, Schematic showing the morphology of an ON-type pyramidal cell with its distinctive basilar dendrite receiving excitatory input from peripheral afferents. Bottom, Sinusoidal EOD AM stimulus with 4 Hz frequency and the spiking response of an example ON-type pyramidal neuron. **B**, Top, Schematic showing the morphology of an OFF-type pyramidal cell. Note the lack of a basilar dendrite as the cell instead receives disinhibitory input from peripheral afferents on its soma through a local interneuron (not shown). Bottom, Sinusoidal EOD AM stimulus with 4 Hz frequency and the spiking response of an example OFF-type pyramidal neuron. **C**, Phase histogram showing the preferred phase response from the same neuron shown in **A** with the best-fit sinusoid (dashed black line). **D**, Phase histogram showing the preferred phase response from the same neuron shown in **B** with the best-fit sinusoid (dashed black line). **E**, Distribution of preferred phases for ON (green) and OFF (red) ELL pyramidal cells in our data set. The entire distribution was clearly bimodal (Hartigan's dip test,  $p = 0.01$ ), and both modes could easily be separated.

observed in the LS (ON,  $\alpha = 0.22 \pm 0.02$ ; OFF,  $\alpha = 0.17 \pm 0.04$ ; one-way ANOVA,  $p = 0.29$ ).

We next investigated how CMS pyramidal cells responded to envelopes. While ON- and OFF-type cells also display similar response profiles, our data show that CMS pyramidal cells respond to envelopes in a qualitatively different manner than their CLS or LS counterparts. This is because we found that response gain was independent of envelope frequency and that these cells displayed little or no phase lead (Fig. 4C, compare filled, open red and green circles). Our data were also well fit

by a fractional differentiation model (Fig. 4C, compare circles, dashed lines), but the obtained fractional differentiation exponents (i.e., the power-law exponent), while similar for ON- and OFF-type cells (ON,  $\alpha = 0.06 \pm 0.05$ ; OFF,  $\alpha = 0.04 \pm 0.04$ ; one-way ANOVA,  $p = 0.82$ ), were not significantly different from zero (ON,  $t$  test,  $p = 0.29$ ; OFF,  $t$  test,  $p = 0.25$ ), indicating that CMS pyramidal cells performed little or no filtering on the envelope stimulus.

Our results thus show that ELL pyramidal cells within all three maps responded to envelopes, thereby providing strong evidence

# Envelopes

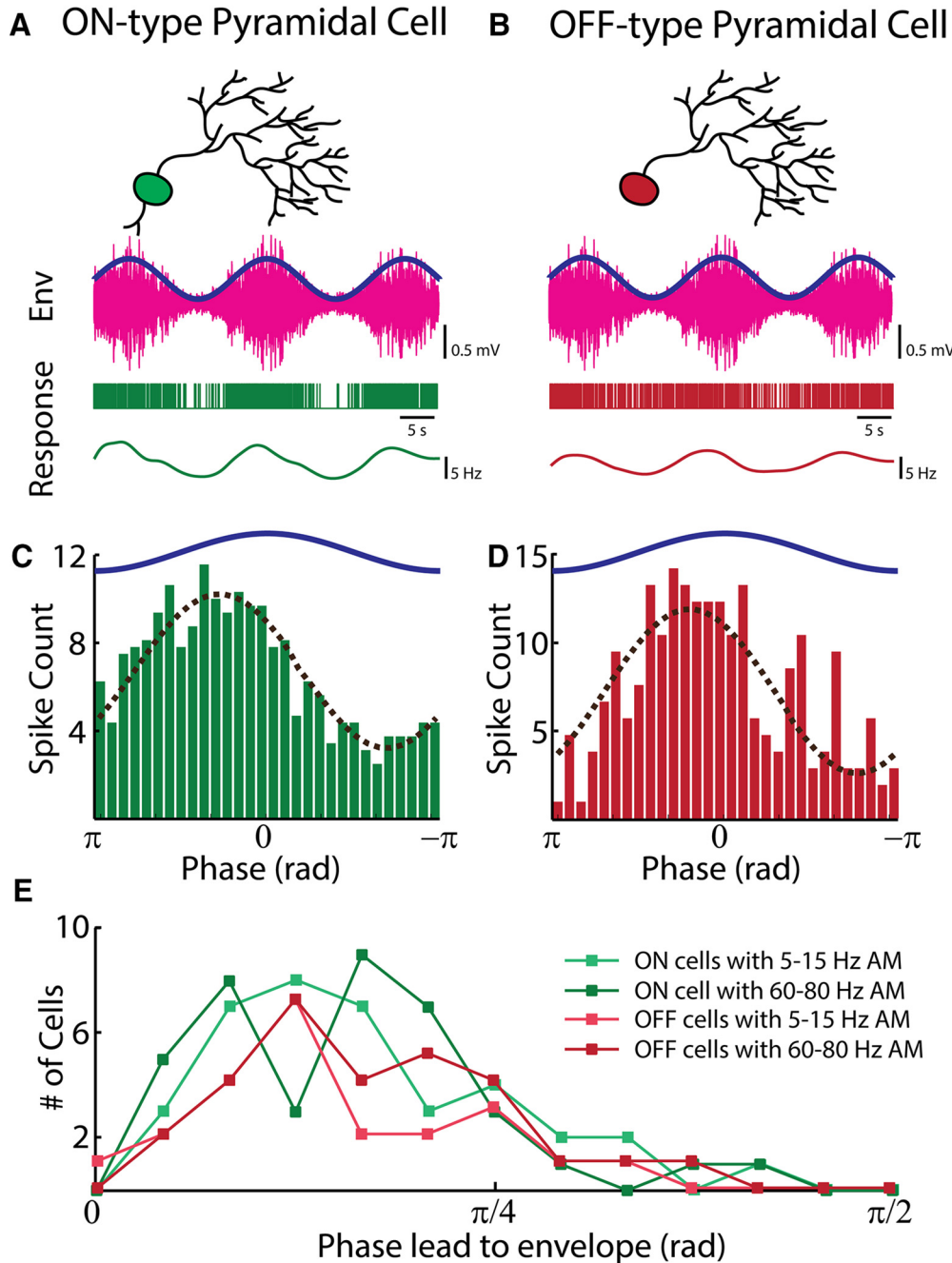


**Figure 3.** ON- and OFF-type pyramidal neurons respond similarly to envelopes (i.e., second order). **A**, Top, Stimulus consisting of a noisy EOD AM (magenta) whose envelope (blue) is modulated sinusoidally. Bottom, Spiking and time-varying firing rate response from an example ON-type LS pyramidal cell to this stimulus. **B**, Top, Stimulus consisting of a noisy EOD AM (magenta) whose envelope (blue) is modulated sinusoidally. Bottom, Spiking and time-varying firing rate response from an example OFF-type LS pyramidal cell to this stimulus. **C**, Phase histogram from the same LS ON-type example neuron shown in **A** to the envelope with the best-fit sinusoid (dashed black line). **D**, Phase histogram from the same LS OFF-type example neuron shown in **B** to the envelope with the best-fit sinusoid (dashed black line). **E**, Distribution of preferred phases for ON (green) and OFF (red) ELL pyramidal cells in our data set across the CMS, CLS, and LS maps for 5–15 Hz (light green and red) and 60–80 Hz (dark green and red) EOD AMs. All distributions were not significantly different from one another (Kruskal–Wallis test,  $p = 0.89$ ).

against the hypothesis that there is only one ELL map that processes these. Rather, pyramidal cells across the ELL maps were differentially tuned to envelopes. We conclude that pyramidal cell heterogeneities across the ELL maps significantly influence their response properties to envelopes. LS pyramidal cell responses displayed the strongest fractional differentiation expo-

nent, followed by their CLS counterparts, with CMS pyramidal performing little or no fractional differentiation (Fig. 4D; one-way ANOVA with Tukey’s LSD correction,  $p < 0.05$ ). We note that since we found no significant differences between ON- and OFF-type cells across all three segments, data from each cell class were pooled in all subsequent analyses.

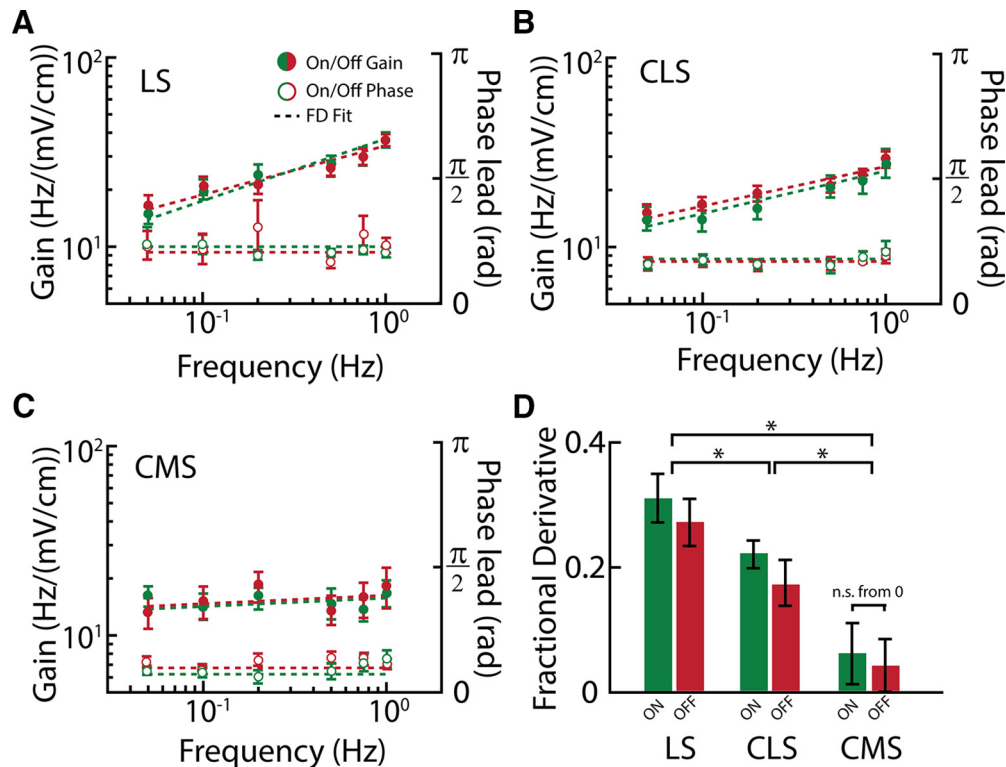


**Figure 4.** ELL pyramidal cells across the three ELL maps display differential responses to envelopes. **A**, Population-averaged gain (filled circles) and phase (open circles) relating the neural response to the envelope for LS ON (green) and OFF (red) pyramidal neurons with fractional differentiation (FD) fits (dashed lines). **B**, **C**, Same as **A** but for CLS and CMS cells, respectively. **D**, Population-averaged fractional differentiation exponents for ON (green) and OFF (red) pyramidal cells in LS (left), CLS (middle), and CMS (right). For each map, the fractional differentiation exponents of ON- and OFF-type cells were not significantly different from one another (one-way ANOVA's,  $p \geq 0.29$  in all three cases). In contrast, the fractional differentiation exponents were significantly different between maps and decreased from LS to CMS. \* $p < 0.05$  (one-way ANOVA with Tukey's LSD correction). Error bars indicate  $\pm 1$  SEM.

**A simple LIF model predicts that differential degrees of adaptation can explain the observed response heterogeneities across ELL maps to second-order electrosensory stimuli**

How can the observed differences between the responses of LS, CLS, and CMS pyramidal cells to envelopes be explained? Previous studies have shown that spike frequency adaptation can lead to high-pass filtering of the neuronal response (Benda et al., 2005; Benda and Hennig, 2008; Deemyad et al., 2012). Importantly, pyramidal cells display spike frequency adaptation in response to envelope steps, with the degree of adaptation strongest in the LS and weakest in the CMS (Zhang and Chacron, 2016). Thus, we hypothesized that the different response profiles across the ELL maps could be explained by the fact that ELL pyramidal cells display different degrees of adaptation. To test this hypothesis, we used a simple model based on the leaky integrate-and-fire formalism that included an adaptation current (Fig. 5A; see Materials and Methods). We found that, with high adaptation, our model could successfully reproduce the gain and phase of LS pyramidal cells (Fig. 5B). By decreasing the adaptation strength in our model, we were able to successfully reproduce the gain and phase of CLS pyramidal cells (Fig. 5C). Finally, with no adaptation, our model successfully reproduced the gain and phase of CMS pyramidal cells (Fig. 5D). In all cases, our model simulation data were well fit by a fractional differentiation model whose exponent matched that observed experimentally (Fig. 5E; LS,  $t$  test,  $p = 0.10$ ; CLS,  $t$  test,  $p = 0.40$ ; CMS,  $t$  test,  $p = 0.73$ ). These results demonstrate that by manipulating the degree of adaptation, we can reproduce the experimentally observed heterogeneities in the responses of ELL pyramidal cells across the three maps.

Our model thus predicts that it is the degree of adaptation that determines a cell's response profile to envelopes.

**Our simple LIF model also predicts that differential degrees of adaptation can explain the observed response heterogeneities within each ELL map**

We next tested whether pyramidal cell class (i.e., superficial, intermediate, or deep) influenced responses to envelopes. To do so, we segregated cells within each segment into deep (LS,  $n = 9$ ; CLS,  $n = 9$ ; CMS,  $n = 10$ ), intermediate (LS,  $n = 12$ ; CLS,  $n = 11$ ; CMS,  $n = 9$ ), and superficial (LS,  $n = 14$ ; CLS,  $n = 8$ ; CMS,  $n = 8$ ) using the baseline firing rate as done previously (Chacron et al., 2005b; Chacron, 2006; Avila-Akerberg et al., 2010). We found that within the LS, superficial cells displayed the greatest degree of fractional differentiation, followed by intermediate cells, with deep cells displaying the least degree of fractional differentiation (Fig. 6A). Qualitatively similar results were obtained in the CLS (Fig. 6B). Importantly, we found that, within the CMS, deep, intermediate, and superficial pyramidal cells all displayed little to no fractional differentiation (Fig. 6C).

We then tested using our model whether differential degrees of adaptation could explain the different levels of fractional differentiation performed by superficial, intermediate, and deep cells across all three ELL maps. We found that by suitably varying the adaptation strength in our model, we could reproduce the response heterogeneities within each segment (Fig. 6, compare circles, squares). We thus conclude that our simple mathematical model could reproduce all the response heterogeneities seen in the data. Our model thus makes the important prediction that the



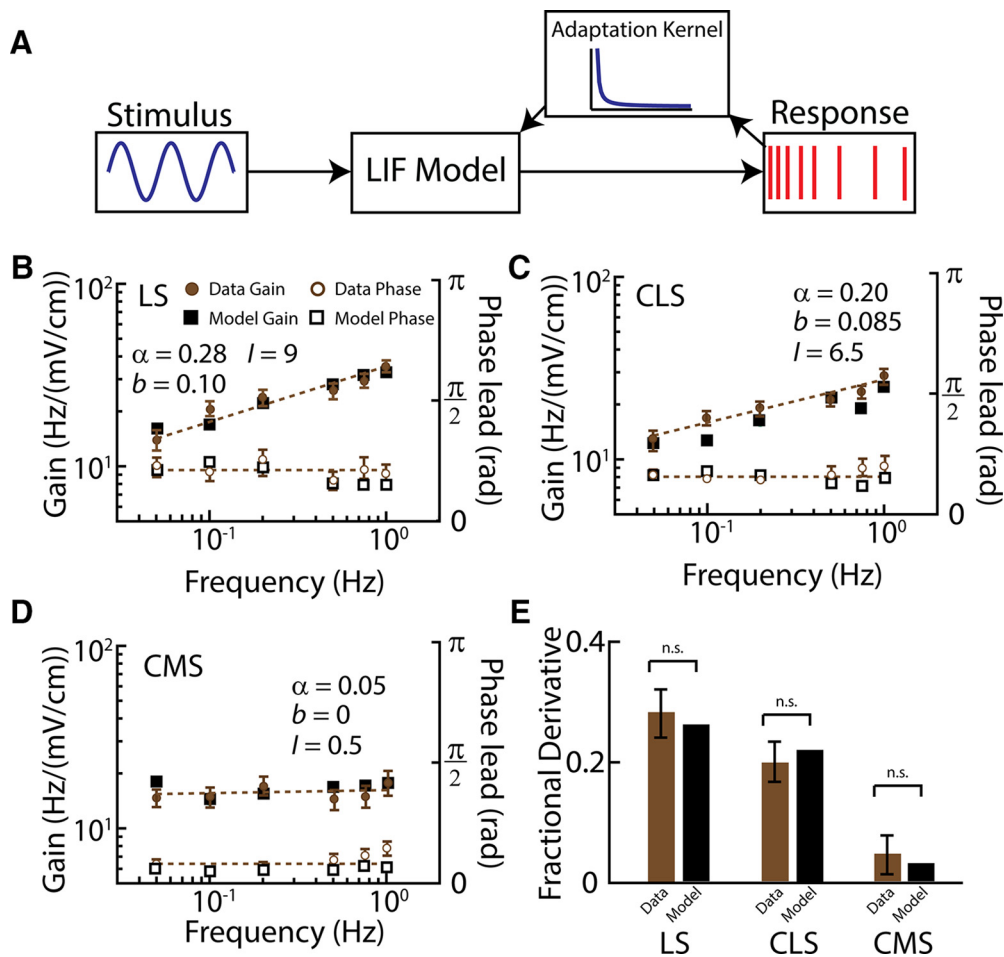


**Figure 5.** A simple leaky integrate-and-fire model with power-law adaptation successfully reproduces the experimentally observed heterogeneities seen across ELL maps. **A**, Model schematic representation in which the stimulus (blue) is fed to an LIF neuron model with an adaptation kernel that decays as a power law as a function of time. We chose a power law since a previous study has shown that LS pyramidal cells displayed power-law adaptation in response to envelope stimuli (Huang et al., 2016). **B**, Population-averaged gain (filled circles) and phase (open circles) for our experimental data in the LS. Also shown are the gain (filled black squares) and phase (open black squares) from our LIF model. **C, D**, Same as **B** but for our CLS and CMS data sets, respectively. Note that  $l$  was decreased to maintain the baseline (i.e., in the absence of stimulation) constant across all segments, as observed experimentally (Krahe et al., 2008). **E**, Population-averaged fractional differentiation exponents for our experimental data (brown) and model (black) for the LS (left), CLS (middle), and CMS (right). For all three maps, the fractional differentiation exponents obtained experimentally and from the model were not significantly different from one another. n.s., Not significant at the  $p < 0.05$  level. Error bars indicate  $\pm 1$  SEM.

differential levels of fractional differentiation seen across ELL maps and across pyramidal cell class can both be explained by differences in the level of adaptation. The implications of this result as well as the nature of the underlying mechanisms are discussed below.

#### Coding of natural envelope stimuli by ELL pyramidal cells

It is important to note that we have, so far, used artificial sinusoidal envelope stimuli to characterize the responses of ELL pyramidal cells across maps. However, natural envelope stimuli are not sinusoidal in nature and are instead characterized by a whole spectrum of temporal frequencies (Yu et al., 2012; Fotowat et al., 2013; Metzner and Chacron, 2014). Importantly, as natural envelope stimuli are scale invariant (i.e., are self-similar when looked at different timescales), their power spectrum decays according to a power law as a function of envelope temporal frequency (Fig. 7A). As mentioned above, to maximize information transmission, a neuron's tuning curve should oppose this decaying power such that response power is independent of frequency (i.e., temporal decorrelation or whitening).

We thus investigated how different ELL pyramidal cell classes (i.e., deep, intermediate, and superficial) across maps (i.e., CMS,

CLS, and LS) responded to natural envelope stimuli. Within the LS, we found that the response power spectra of superficial pyramidal cells were independent of frequency (Fig. 7B, top). That of intermediate pyramidal cells decayed as a function of frequency (Fig. 7B, middle), while that of deep pyramidal cells showed an even more pronounced decay (Fig. 7B, bottom). We quantified the degree of temporal decorrelation or whitening by computing a white index whose value is 1 if the response power spectrum is constant. White index values were greatest for LS superficial pyramidal cells, followed by intermediate pyramidal cells, and smallest for deep pyramidal cells (Fig. 7E).

In contrast, superficial cells within the CLS did not perform as much temporal decorrelation of natural envelope stimuli as their LS counterparts, as quantified by a lower white index (Fig. 7C, top). Superficial CLS pyramidal cells nevertheless displayed larger white index values than their intermediate counterparts (Fig. 7C, compare top, middle panels). Deep CLS cells performed even less temporal decorrelation (Fig. 7C, bottom). Interestingly, superficial, intermediate, and deep CMS pyramidal cells did not perform any significant temporal decorrelation or whitening of natural envelope stimuli (Fig. 7D, top, middle, bottom, E). Indeed, the white index values computed from the neural responses



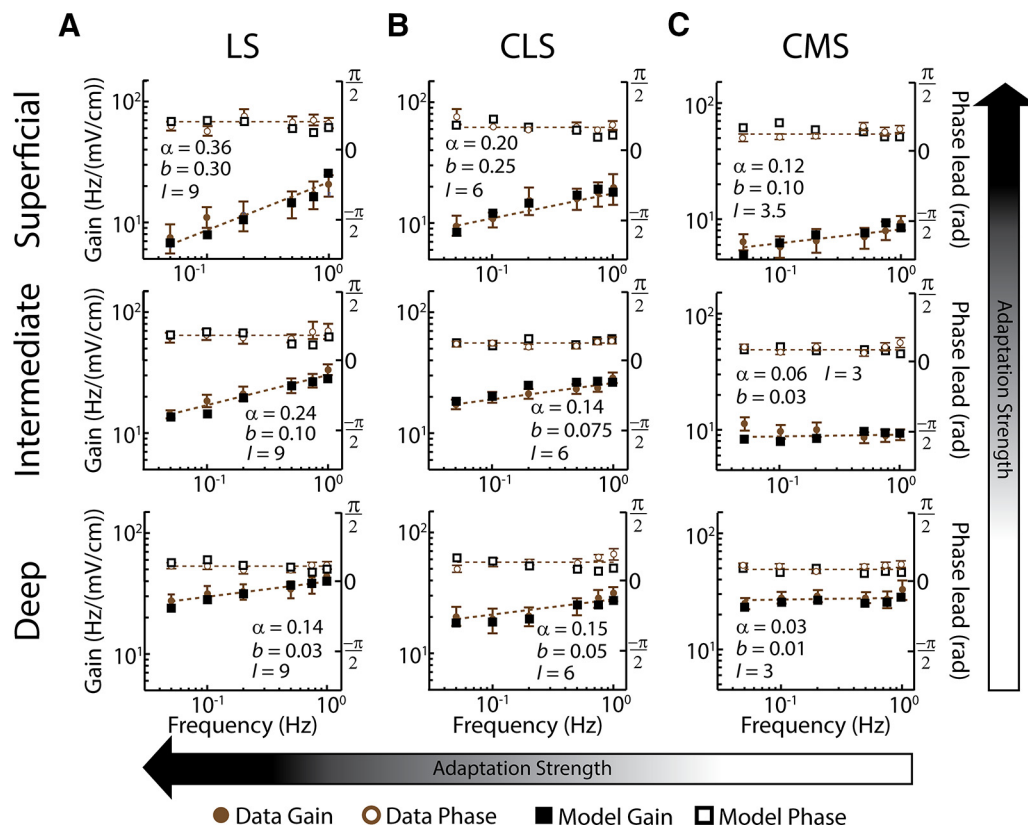


**Figure 6.** Pyramidal cell classes within each ELL map display differential responses to envelopes. **A**, Population-averaged gain (filled brown circles) and phase (open brown circles) for our experimental data for superficial (top), intermediate (middle), and deep (bottom) LS cells. Also shown are the gain (filled black squares) and phase (open black squares) from the model in each case with corresponding fractional differentiation exponent  $\alpha$  and adaptation strength value  $b$ . **B**, **C**, same as **A**, but for CLS and CMS neurons, respectively. Note that for the CMS, deep, intermediate, and superficial neurons all displayed similar fractional differentiation exponents that were all not significantly different from 0. Our LIF model could reproduce heterogeneities in envelope responses by decreasing adaptation strength going from the LS to CMS for a given cell class (i.e., deep, intermediate, or superficial) as well as going from superficial to deep within a given ELL map (i.e., CMS, CLS, or LS). The values of model parameters  $b$  and  $l_{bias}$  (in microamperes per square centimeter) used in each case are shown.

were not significantly different from those obtained for the stimulus power spectrum (Fig. 7E), indicating that these cells instead preserve the statistics of natural input in their responses.

**Summary**

Figure 8 shows a summary of our results. A previous study has shown that most peripheral receptors do not perform significant filtering of envelopes and thus faithfully relay information about their detailed structure to ELL pyramidal cells (Metzen and Chacron, 2015). Overall, ON- and OFF-type pyramidal cells displayed similar responses to envelopes. Using artificial sinusoidal envelopes, we further found that LS cells displayed, on average, the strongest degree of fractional differentiation to envelope stimuli. CLS cells displayed, on average, intermediate degrees of fractional differentiation, while CMS cells displayed little or no fractional differentiation (Fig. 8). Within the CLS and LS segments, deep pyramidal cells performed little to no fractional differentiation while superficial pyramidal cells displayed the greatest degree of fractional differentiation. Overall, a mathematical model showed that differential levels of adaptation could explain the experimentally observed heterogeneities in tuning. Using natural stimuli, we found that superficial pyramidal cells within the LS and CLS performed temporal decorrelation or whitening, while all CMS cells instead preserved natural stimulus statistics. Thus, our results show that a significant proportion of ELL pyramidal cells (deep cells for the LS and CLS as well as all cells within CMS) perform little to no filtering of envelope stim-

uli. As all pyramidal cells project to higher brain areas, our results have important implications for understanding envelope coding as discussed further below.

**Discussion**

**ELL pyramidal cell heterogeneities and coding of second-order electrosensory attributes**

We investigated how ELL pyramidal cell heterogeneities influence their responses to envelopes. We found that heterogeneities either did not influence or strongly influenced envelope responses. Specifically, the responses of ON- and OFF-type ELL pyramidal cells, despite being out of phase with one another when first-order electrosensory stimulus features were considered, were actually in phase with one another when second-order electrosensory stimulus features were instead considered. Such relative homogeneity is surprising given that peripheral afferents providing feedforward input to ELL pyramidal cells display strong heterogeneities in their responses to second-order features (Savard et al., 2011; Metzen and Chacron, 2015). Indeed, responses to envelopes were in phase for 66% of afferents and out of phase for the remaining 34%. One possibility is that afferents whose responses are out of phase with the envelope do not synapse directly onto pyramidal cells, but rather indirectly through local inhibitory interneurons, thereby making the input in phase with the envelope and potentially explaining why ON- and OFF-type ELL pyramidal cells display similar responses to envelopes.

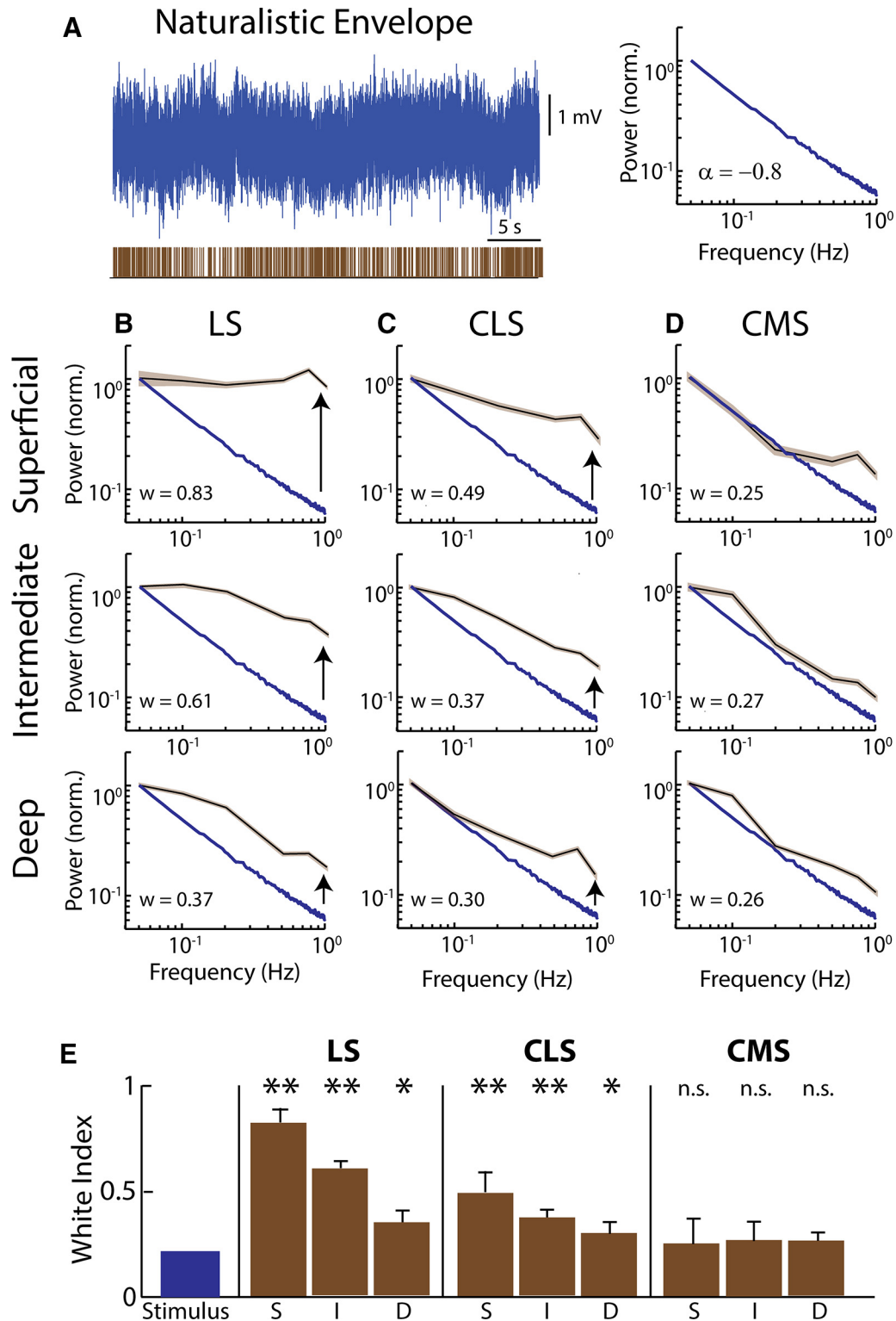


**Figure 7.** Different pyramidal cell classes across the three ELL maps perform different degrees of temporal whitening in response to natural envelope stimuli. **A**, Example time series of a natural envelope stimulus (top left), its power spectrum (top right) that decays as a power law with exponent  $-0.8$  as a function of temporal frequency, and the spiking response from an example pyramidal neuron (bottom left). **B**, Stimulus (blue) and population-averaged response (black) power spectra for superficial (top), intermediate (middle), and deep (bottom) LS pyramidal cells. **C**, **D**, same as **B**, but for CLS and CMS pyramidal cells, respectively. **E**, Population-averaged whitening indices for the stimulus (blue) and for superficial (S), intermediate (I), and deep (D) pyramidal cells within the LS (left), CLS (middle), and CMS (right) maps. \* $p < 0.05$ ; \*\* $p < 0.01$ . n.s., Not significant at the  $p < 0.05$  level. Error bars indicate  $\pm 1$  SEM.

We also found that responses to envelopes were cell class (i.e., superficial, intermediate, or deep) as well as map specific. However, as the connectivity pattern from ELL to torus semicircularis (TS), while preserving somatotopy, appears to be random with respect to

cell class or map (Krahe and Maler, 2014), we argue that the different envelope response profiles observed in ELL constitute heterogeneities from the point of view of the decoder. Our simple mathematical model further showed that different levels of adaptation could re-

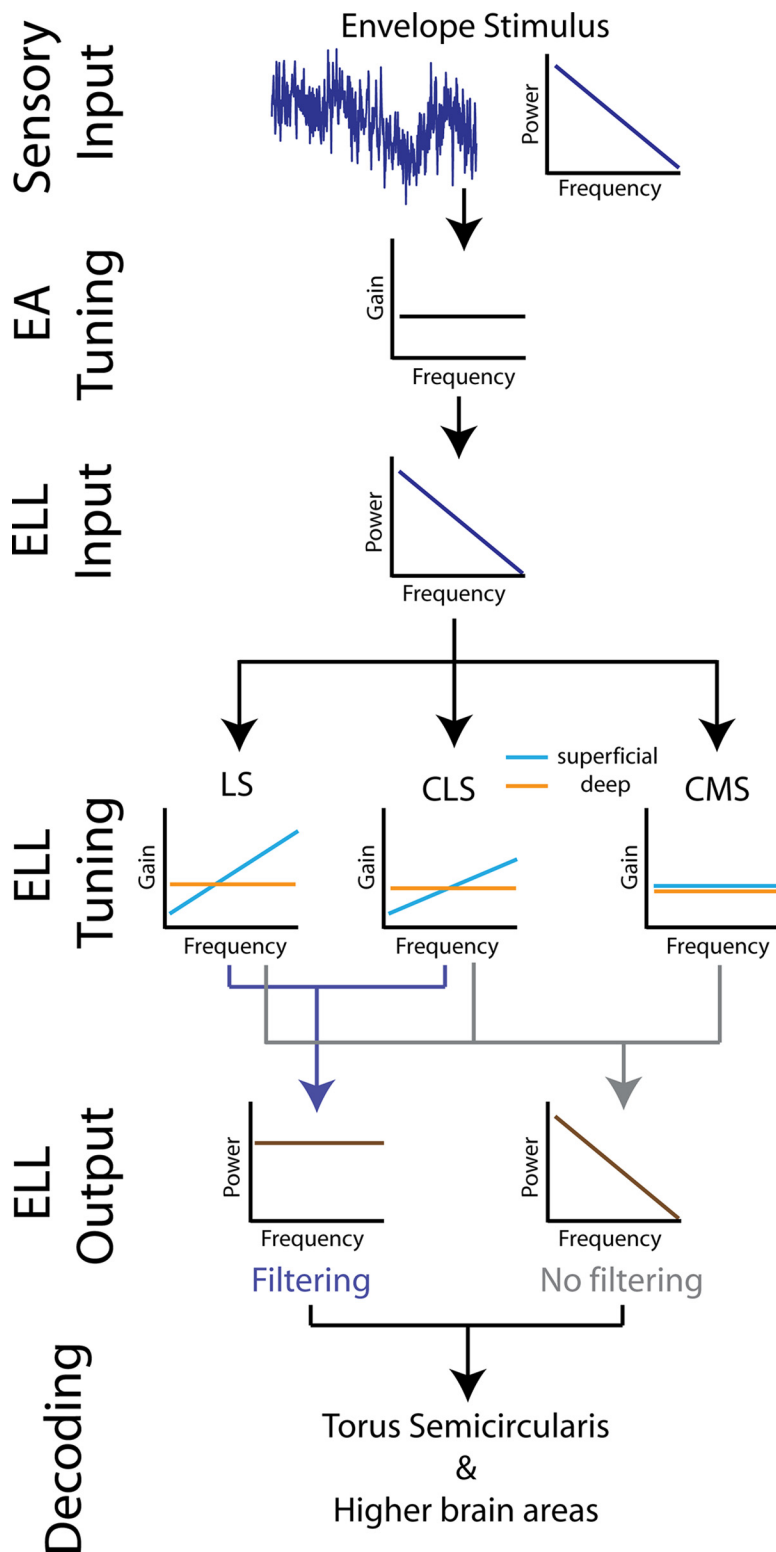


**Figure 8.** Summary of envelope processing by ELL pyramidal neurons. Natural envelope stimuli are first processed by peripheral electroreceptor afferents (EAs) that perform little to no filtering (Metzen and Chacron, 2015), thereby preserving stimulus statistics. EAs then relay this information to pyramidal cells within the three ELL maps. Superficial pyramidal cells (cyan) within the LS perform the most temporal whitening of these natural stimuli (middle left), followed by superficial CLS pyramidal neurons (middle). Within the CMS, all cells display little to no temporal whitening and instead preserve natural envelope stimulus statistics. ELL pyramidal cells can thus be segregated into two groups: those that do not perform filtering (gray) and those that do (navy blue). Information transmitted by those two groups is decoded by TS neurons before being transmitted to higher brain areas.

produce our experimental data. Importantly, our model predicts a strong correlation between the observed fractional differentiation exponent and the strength of adaptation across cell classes and across ELL maps. A previous study has shown that LS pyramidal cells display stronger adaptation to envelope steps than their CMS counterparts (Zhang and Chacron, 2016), thereby supporting our hypothesis. We further hypothesize that the differences in envelope response profiles observed across ELL maps and cell classes are both primarily if not exclusively due to differences in the level of SK channel expression. This is because (1) SK channels strongly influence adaptation in ELL pyramidal cells (Ellis et al., 2007; Deemyad et al., 2012), and (2) the strongest SK channel expression in pyramidal cells was observed in the LS and decreased going to the CLS, with the CMS showing little to no expression (Ellis et al., 2007, 2008). Moreover, within the LS and CLS, the strongest level of SK channel expression was observed for superficial pyramidal cells, decreased for intermediate pyramidal cells, and was almost negligible for deep pyramidal cells (Maler, 2009). Thus, experimentally observed variations in the fractional differentiation exponent were very well correlated with known levels of SK channel expression across cell classes and across ELL maps. Together with previous results showing that pharmacological manipulation of SK channels can directly alter LS pyramidal cell tuning to envelopes (Huang et al., 2016), these results strongly suggest that SK channel expression determines a pyramidal cell’s response to envelopes.

ELL pyramidal cell receptive fields (RFs) have a classic antagonistic center-surround organization. There is a trade-off between the relative sizes of the RF center and surround across the ELL maps. Indeed, while RF center size decreases from CMS to LS, RF surround size instead increases (Shumway, 1989; Maler, 2009). Moreover, superficial cells have the largest surround, while deep cells have little to no surround (Bastian et al., 2002). Thus, while RF size differences across maps are linked to differences in tuning to AM temporal frequency (for review, see Krahe and Maler, 2014), there does not appear to be such a link when envelopes are instead considered. One important caveat, however, is that ELL pyramidal cell RFs were all measured using AMs and not envelopes. Further studies are needed to map pyramidal cell RFs to envelopes and determine whether the spatial structure is coordinated with the temporal response profile.

### Functional role of pyramidal cell heterogeneities in coding of first- and second-order electrosensory stimulus attributes

Our results have shown that, within the LS and CLS segments, deep pyramidal cells performed little to no filtering of envelope stimuli, as indicated by their gains that were independent of envelope frequency and negligible phase leads. As such, their responses closely resembled those of most peripheral afferents (Metzen and Chacron, 2015). An important question is thus, what is the functional role of having central neurons whose responses are virtually identical to those of most peripheral receptors? One potential explanation is that deep cells exclusively project to the nucleus praeminentialis and provide feedback to their superficial and intermediate counterparts indirectly via parallel fibers originating from cerebellar granule cells within the eminentia granularis posterior (Bastian et al., 2004). We hypothesize that the lack of filtering by LS and CLS deep cells is necessary to provide feedback to their superficial and intermediate counterparts, thereby determining their response properties to envelopes.

Interestingly, all pyramidal cells within the CMS performed no significant filtering of envelope stimuli because their gains did not depend on envelope frequency and they displayed negligible phase leads. As such, their response profiles closely resemble those of most peripheral receptor afferents (Metzen and Chacron, 2015). What is then the functional role of CMS pyramidal neurons in envelope processing? One possibility is that the observed responses to envelopes are not behaviorally relevant, as downstream brain areas do not decode them. While this possibility cannot be ruled out, we argue that it is unlikely to be true. First, the CMS is by far the largest segment and it does not appear efficient to effectively “waste” such a large amount of resources on the coding of behaviorally relevant stimuli. Rather, as all three ELL maps project to downstream brain areas such as the mid-brain TS, we hypothesize that the responses of CMS cells are necessary to properly decode the filtered responses of superficial and intermediate LS and CLS pyramidal cells. The lack of fractional differentiation observed for CMS neurons could provide the contextual information necessary to properly decode the optimized representation of natural envelope stimuli provided by superficial LS pyramidal neurons in downstream areas.

Alternatively, it is also possible that the lack of filtering by CMS pyramidal cells serves to provide reliable responses to the prominent low-frequency components of natural envelope stimuli, while the high-pass filtering through fractional differentiation would serve to enhance responses to the weak high-frequency components that could easily be contaminated by noise, as proposed originally by Barlow (2001). We note that such high-pass filtering cannot extend to arbitrarily large frequencies where stimulus power is negligible, as it would then lead to noise magnification. As such, neural sensitivity should increase over the frequency range for which stimulus power is significant and decrease for higher frequencies. Such bandpass tuning has been observed in the retina and is thought to provide an efficient strategy for coding natural scenes (Atick and Redlich, 1992). In the electrosensory system, natural envelopes can contain significant power for frequencies up to  $\sim 10$  Hz (Stamper et al., 2012, 2013; Fotowat et al., 2013). Further studies using envelope frequencies higher than those used here are needed to test whether the sensitivity of ELL pyramidal cells to these will decrease. It is also possible that neurons in higher brain areas low-pass filter input from ELL pyramidal cells, thereby removing noise. Further studies focusing on how TS neurons receiving input from ELL pyramidal cells are tuned to envelopes are necessary to test this hypothesis and are beyond the scope of this paper. However, we note that previous studies have

found that a significant fraction of TS neurons displayed responses that were similar to that of ELL neurons and that these project to higher brain areas (Vonderschen and Chacron, 2011; Sproule et al., 2015). It is thus very likely that the information transmitted by CMS pyramidal cells about envelopes is preserved in the electrosensory brain and contributes to determining observed behavioral responses (Metzen and Chacron, 2014).

### Implications for other systems

It is likely that our results will be applicable to other systems. First, we note that natural stimuli across sensory modalities frequently consist of a fast time-varying waveform whose envelope varies more slowly. For example, in the auditory system, envelopes carry behaviorally relevant information relating to timbre for music as well as speech recognition (Shannon et al., 1998; Heil, 2003) and are also characterized by a power spectrum that decays as a power law (Theunissen and Elie, 2014). Studies of auditory processing of natural sounds suggest that the auditory system efficiently encodes them through whitening (Lewicki, 2002; Rodriguez et al., 2010). Other sensory systems also perform whitening of natural stimuli (Dan et al., 1996; Wang et al., 2003), and our proposed mechanism involving SK channels, which are expressed ubiquitously in the CNS and are major determinants of adaptation (Adelman et al., 2012), could explain the observed high-pass filtering properties of these sensory neurons to artificial stimuli, thereby explaining whitened responses to natural stimuli whose spectra decay as a function of frequency.

### References

- Adelman JP, Maylie J, Sah P (2012) Small-conductance Ca<sup>2+</sup>-activated K<sup>+</sup> channels: form and function. *Annu Rev Physiol* 74:245–269. [CrossRef Medline](#)
- Atick JJ, Redlich A (1992) What does the retina know about natural scenes. *Neural Comput* 4:196–211. [CrossRef](#)
- Attneave F (1954) Some Informational Aspects of Visual Perception. *Psychol Rev* 61:183–193. [CrossRef Medline](#)
- Aumentado-Armstrong T, Metzen MG, Sproule MK, Chacron MJ (2015) Electrosensory midbrain neurons display feature invariant responses to natural communication stimuli. *PLoS Comput Biol* 11:e1004430. [CrossRef Medline](#)
- Avila-Akerberg O, Krahe R, Chacron MJ (2010) Neural heterogeneities and stimulus properties affect burst coding *in vivo*. *Neuroscience* 168:300–313. [CrossRef Medline](#)
- Bannister NJ, Larkman AU (1995a) Dendritic morphology of CA1 pyramidal neurones from the rat hippocampus: II. Spine distributions. *J Comp Neurol* 360:161–171. [CrossRef Medline](#)
- Bannister NJ, Larkman AU (1995b) Dendritic morphology of CA1 pyramidal neurones from the rat hippocampus: I. Branching patterns. *J Comp Neurol* 360:150–160. [CrossRef Medline](#)
- Barlow H (2001) Redundancy reduction revisited. *Network* 12:241–253. [CrossRef Medline](#)
- Barlow HB (1961) Possible principles underlying the transformation of sensory messages. In: *Sensory communication* (Rosenblith W, ed), pp 217–234. Cambridge, MA: MIT.
- Bastian J, Nguyenkim J (2001) Dendritic modulation of burst-like firing in sensory neurons. *J Neurophysiol* 85:10–22. [Medline](#)
- Bastian J, Chacron MJ, Maler L (2002) Receptive field organization determines pyramidal cell stimulus-encoding capability and spatial stimulus selectivity. *J Neurosci* 22:4577–4590. [Medline](#)
- Bastian J, Chacron MJ, Maler L (2004) Plastic and non-plastic cells perform unique roles in a network capable of adaptive redundancy reduction. *Neuron* 41:767–779. [CrossRef Medline](#)
- Benda J, Hennig RM (2008) Spike-frequency adaptation generates intensity invariance in a primary auditory interneuron. *J Comput Neurosci* 24:113–136. [CrossRef Medline](#)
- Benda J, Longtin A, Maler L (2005) Spike-frequency adaptation separates transient communication signals from background oscillations. *J Neurosci* 25:2312–2321. [CrossRef Medline](#)



- Chacron MJ (2006) Nonlinear information processing in a model sensory system. *J Neurophysiol* 95:2933–2946. [CrossRef Medline](#)
- Chacron MJ, Doiron B, Maler L, Longtin A, Bastian J (2003) Non-classical receptive field mediates switch in a sensory neuron's frequency tuning. *Nature* 423:77–81. [CrossRef Medline](#)
- Chacron MJ, Longtin A, Maler L (2005a) Delayed excitatory and inhibitory feedback shape neural information transmission. *Physical Review E* 72:051917. [CrossRef](#)
- Chacron MJ, Maler L, Bastian J (2005b) Feedback and feedforward control of frequency tuning to naturalistic stimuli. *J Neurosci* 25:5521–5532. [CrossRef Medline](#)
- Chacron MJ, Longtin A, Maler L (2011) Efficient computation via sparse coding in electrosensory neural networks. *Curr Opin Neurobiol* 21:752–760. [CrossRef Medline](#)
- Dan Y, Atick JJ, Reid RC (1996) Efficient coding of natural scenes in the lateral geniculate nucleus: experimental test of a computational theory. *J Neurosci* 16:3351–3362. [Medline](#)
- Deemyad T, Kroeger J, Chacron MJ (2012) Sub- and suprathreshold adaptation currents have opposite effects on frequency tuning. *J Physiol* 590:4839–4858. [CrossRef Medline](#)
- Deemyad T, Metzzen MG, Pan Y, Chacron MJ (2013) Serotonin selectively enhances perception and sensory neural responses to stimuli generated by same-sex conspecifics. *Proc Natl Acad Sci U S A* 110:19609–19614. [CrossRef Medline](#)
- Drew PJ, Abbott LF (2006) Models and properties of power-law adaptation in neural systems. *J Neurophysiol* 96:826–833. [CrossRef Medline](#)
- Ellis LD, Mehaffey WH, Harvey-Girard E, Turner RW, Maler L, Dunn RJ (2007) SK channels provide a novel mechanism for the control of frequency tuning in electrosensory neurons. *J Neurosci* 27:9491–9502. [CrossRef Medline](#)
- Ellis LD, Maler L, Dunn RJ (2008) Differential distribution of SK channel subtypes in the brain of the weakly electric fish *Apteronotus leptorhynchus*. *J Comp Neurol* 507:1964–1978. [CrossRef Medline](#)
- Fotowat H, Harrison RR, Krahe R (2013) Statistics of the electrosensory input in the freely swimming weakly electric fish *Apteronotus leptorhynchus*. *J Neurosci* 33:13758–13772. [CrossRef Medline](#)
- Frank K, Becker MC (1964) Microelectrodes for recording and stimulation. In: *Physical techniques in biological research* (Nastuk WL, ed), pp 23–84. New York: Academic.
- Goldberg JM (2000) Afferent diversity and the organisation of central vestibular pathways. *Exp Brain Res* 130:277–297. [CrossRef Medline](#)
- Heil P (2003) Coding of temporal onset envelope in the auditory system. *Speech Commun* 41:123–134. [CrossRef](#)
- Hitschfeld EM, Stamper SA, Vonderschen K, Fortune ES, Chacron MJ (2009) Effects of restraint and immobilization on electrosensory behaviors of weakly electric fish. *ILAR J* 50:361–372. [CrossRef Medline](#)
- Huang CG, Zhang ZD, Chacron MJ (2016) Temporal decorrelation by SK channels enables efficient neural coding and perception of natural stimuli. *Nat Commun* 7:11353. [CrossRef Medline](#)
- Khosravi-Hashemi N, Chacron MJ (2014) Motion processing across multiple topographic maps in the electrosensory system. *Physiol Rep* 2:e00253. [Medline](#)
- Krahe R, Maler L (2014) Neural maps in the electrosensory system of weakly electric fish. *Curr Opin Neurobiol* 24:13–21. [CrossRef Medline](#)
- Krahe R, Bastian J, Chacron MJ (2008) Temporal processing across multiple topographic maps in the electrosensory system. *J Neurophysiol* 100:852–867. [CrossRef Medline](#)
- Lapicque L (1907) Recherches quantitatives sur l'excitation électrique des nerfs traitée comme une polarisation. *J Physiol Pathol Genet* 9:620–635.
- Laughlin S (1981) A simple coding procedure enhances a neuron's information capacity. *Z Naturforsch C* 36:910–912. [Medline](#)
- Lewicki MS (2002) Efficient coding of natural sounds. *Nat Neurosci* 5:356–363. [CrossRef Medline](#)
- Lundstrom BN, Higgs MH, Spain WJ, Fairhall AL (2008) Fractional differentiation by neocortical pyramidal neurons. *Nat Neurosci* 11:1335–1342. [CrossRef Medline](#)
- Maler L (1979) The posterior lateral line lobe of certain gymnotiform fish. Quantitative light microscopy. *J Comp Neurol* 183:323–363. [CrossRef Medline](#)
- Maler L (2009) Receptive field organization across multiple electrosensory maps. I. Columnar organization and estimation of receptive field size. *J Comp Neurol* 516:376–393. [CrossRef Medline](#)
- Maler L, Sas EK, Rogers J (1981) The cytology of the posterior lateral line lobe of high frequency weakly electric fish (*Gymnotidae*): differentiation and synaptic specificity in a simple cortex. *J Comp Neurol* 195:87–139. [CrossRef Medline](#)
- Marder E, Goaillard JM (2006) Variability, compensation and homeostasis in neuron and network function. *Nat Rev Neurosci* 7:563–574. [CrossRef Medline](#)
- Marsat G, Longtin A, Maler L (2012) Cellular and circuit properties supporting different sensory coding strategies in electric fish and other systems. *Curr Opin Neurobiol* 22:686–692. [CrossRef Medline](#)
- McGillivray P, Vonderschen K, Fortune ES, Chacron MJ (2012) Parallel coding of first- and second-order stimulus attributes by midbrain electrosensory neurons. *J Neurosci* 32:5510–5524. [CrossRef Medline](#)
- Mehaffey WH, Maler L, Turner RW (2008) Intrinsic frequency tuning in ELL pyramidal cells varies across electrosensory maps. *J Neurophysiol* 99:2641–2655. [CrossRef Medline](#)
- Mejias JF, Longtin A (2012) Optimal heterogeneity for coding in spiking neural networks. *Phys Rev Lett* 108:228102. [CrossRef Medline](#)
- Metzen MG, Chacron MJ (2014) Weakly electric fish display behavioral responses to envelopes naturally occurring during movement: implications for neural processing. *J Exp Biol* 217:1381–1391. [CrossRef Medline](#)
- Metzen MG, Chacron MJ (2015) Neural heterogeneities determine response characteristics to second-, but not first-order stimulus features. *J Neurosci* 35:3124–3138. [CrossRef Medline](#)
- Metzen MG, Jamali M, Carriot J, Ávila-Åkerberg O, Cullen KE, Chacron MJ (2015) Coding of envelopes by correlated but not single-neuron activity requires neural variability. *Proc Natl Acad Sci U S A* 112:4791–4796. [CrossRef Medline](#)
- Metzen MG, Hofmann V, Chacron MJ (2016) Neural correlations enable invariant coding and perception of natural stimuli in weakly electric fish. *Elife* 5:e12993. [Medline](#)
- Metzner W, Juranek J (1997) A sensory brain map for each behavior? *Proc Natl Acad Sci U S A* 94:14798–14803. [CrossRef Medline](#)
- Middleton JW, Longtin A, Benda J, Maler L (2006) The cellular basis for parallel neural transmission of a high-frequency stimulus and its low-frequency envelope. *Proc Natl Acad Sci U S A* 103:14596–14601. [CrossRef Medline](#)
- Padmanabhan K, Urban NN (2010) Intrinsic biophysical diversity decorrelates neuronal firing while increasing information content. *Nat Neurosci* 13:1276–1282. [CrossRef Medline](#)
- Pozzorini C, Naud R, Mensi S, Gerstner W (2013) Temporal whitening by power-law adaptation in neocortical neurons. *Nat Neurosci* 16:942–948. [CrossRef Medline](#)
- Rieke F, Warland D, de Ruyter van Steveninck RR, Bialek W (1996) *Spikes: exploring the neural code*. Cambridge, MA: MIT.
- Rodriguez FA, Chen C, Read HL, Escabi MA (2010) Neural modulation tuning characteristics scale to efficiently encode natural sound statistics. *J Neurosci* 30:15969–15980. [CrossRef Medline](#)
- Saunders J, Bastian J (1984) The physiology and morphology of two classes of electrosensory neurons in the weakly electric fish *Apteronotus leptorhynchus*. *J Comp Physiol A Neuroethol Sens Neural Behav Physiol* 154:199–209. [CrossRef](#)
- Savard M, Krahe R, Chacron MJ (2011) Neural heterogeneities influence envelope and temporal coding at the sensory periphery. *Neuroscience* 172:270–284. [CrossRef Medline](#)
- Schulz DJ, Goaillard JM, Marder E (2006) Variable channel expression in identified single and electrically coupled neurons in different animals. *Nat Neurosci* 9:356–362. [CrossRef Medline](#)
- Shannon RV, Zeng FG, Wyganski J (1998) Speech recognition with altered spectral distribution of envelope cues. *J Acoust Soc Am* 104:2467–2476. [CrossRef Medline](#)
- Shumway CA (1989) Multiple electrosensory maps in the medulla of weakly electric gymnotiform fish. I. Physiological differences. *J Neurosci* 9:4388–4399. [Medline](#)
- Simmonds B, Chacron MJ (2015) Activation of parallel fiber feedback by spatially diffuse stimuli simultaneously reduces signal and noise correlations via independent mechanisms in a cerebellum-like structure. *PLoS Comp Biol* 11:e1004034. [CrossRef](#)
- Simoncelli EP, Olshausen BA (2001) Natural image statistics and neural representation. *Annu Rev Neurosci* 24:1193–1216. [CrossRef Medline](#)
- Sproule MK, Metzzen MG, Chacron MJ (2015) Parallel sparse and dense

- information coding streams in the electrosensory midbrain. *Neurosci Lett* 607:1–6. [CrossRef Medline](#)
- Stamper SA, Madhav MS, Cowan NJ, Fortune ES (2012) Beyond the jamming avoidance response: weakly electric fish respond to the envelope of social electrosensory signals. *J Exp Biol* 215:4196–4207. [CrossRef Medline](#)
- Stamper SA, Fortune ES, Chacron MJ (2013) Perception and coding of envelopes in weakly electric fishes. *J Exp Biol* 216:2393–2402. [CrossRef Medline](#)
- Theunissen FE, Elie JE (2014) Neural processing of natural sounds. *Nat Rev Neurosci* 15:355–366. [CrossRef Medline](#)
- Toporikova N, Chacron MJ (2009) Dendritic SK channels gate information processing *in vivo* by regulating an intrinsic bursting mechanism seen *in vitro*. *J Neurophysiol* 102:2273–2287. [CrossRef Medline](#)
- Tripathy SJ, Padmanabhan K, Gerkin RC, Urban NN (2013) Intermediate intrinsic diversity enhances neural population coding. *Proc Natl Acad Sci U S A* 110:8248–8253. [CrossRef Medline](#)
- Vonderschen K, Chacron MJ (2011) Sparse and dense coding of natural stimuli by distinct midbrain neuron subpopulations in weakly electric fish. *J Neurophysiol* 106:3102–3118. [CrossRef Medline](#)
- Wang XJ, Liu Y, Sanchez-Vives MV, McCormick DA (2003) Adaptation and temporal decorrelation by single neurons in the primary visual cortex. *J Neurophysiol* 89:3279–3293. [CrossRef Medline](#)
- Yu N, Hupe GJ, Garfinkle C, Lewis JE, Longtin A (2012) Coding conspecific identity and motion in the electric sense. *PLoS Comp Biol* 8:e1002564. [CrossRef](#)
- Zhang ZD, Chacron MJ (2016) Adaptation to second order stimulus features by electrosensory neurons causes ambiguity. *Sci Rep* 6:28716. [CrossRef Medline](#)